Analysis of zinc-fingers and homeoboxes (ZHX)-1-interacting proteins: molecular cloning and characterization of a member of the ZHX family, ZHX3

Kazuya YAMADA*†[1], Hiroko KAWATA†, Zhangfei SHOU*, Satoko HIRANO*, Tetsuya MIZUTANI*†, Takashi YAZAWA*†, Toshio SEKIGUCHI*†, Miki YOSHINO*†, Takashi KAJITANI*† and Kaoru MIYAMOTO*†

*Department of Biochemistry, Fukui Medical University, 23-3 Shimoaizuki, Matsuoka-cho, Fukui 910-1193, Japan, and †CREST, Japan Science and Technology, Fukui 910-1193, Japan

Human zinc-fingers and homeoboxes (ZHX) 1, a transcriptional repressor, was originally cloned as an interacting protein with the activation domain of the A subunit of nuclear factor-Y (NF-YA). As the first step in investigating the mechanism by which ZHX1 acts as a transcriptional repressor, we conducted a search of ZHX1-interacting proteins using a yeast two-hybrid system. Nuclear proteins such as ZHX1, transcriptional co-factors and DNA-binding proteins, zyxin, androgen-induced aldose reductase and eleven-nineteen lysine-rich leukaemia gene, as well as some unknown proteins, were cloned. Molecular cloning and determination of the nucleotide sequence of the full-length cDNA encoding a novel protein revealed that it consists of 956 amino acid residues and contains two zinc-finger (Znf) motifs and five homeodomains (HDs) as well as ZHX1. We concluded that the protein forms the ZHX family with ZHX1 and denoted it ZHX3. ZHX3 not only dimerizes with both ZHX1 and ZHX3, but also interacts with the activation domain of the NF-YA. Further analysis revealed that ZHX3 is a ubiquitous transcriptional repressor that is localized in nuclei and functions as a dimer. Lastly, the dimerization domain, the interaction domain with NF-YA, and the repressor domain are mapped to a region including the HD1 region, and two nuclear localization signals are mapped to the N-terminal through Znf1 and the HD2 region, respectively.

Key words: cDNA cloning, nuclear localization, transcriptional repressor, two-hybrid system, zinc-fingers and homeoboxes (ZHX) family.

INTRODUCTION

Nuclear factor-Y (NF-Y), a ubiquitous transcription factor, binds to the Y box sequence (an inverted CCAAT box, 5′-ATTGG-3′) and stimulates transcription from many gene promoters [1]. It consists of three subunits, NF-YA, NF-YB and NF-YC, all of which are necessary for DNA binding [1]. NF-YB and NF-YC interact tightly with each other and their association precedes the association with NF-YA and binding to the cognate DNA sequences [1]. The stable expression of the dominant negative NF-YA that interacts with both NF-YB and NF-YC but is not able to bind to the cognate nucleotide sequence led to retarded cell growth in mouse fibroblast cells, suggesting that NF-Y plays an important role in cell growth [2].

Transcription of the rat pyruvate kinase M (*PKM*) gene is silent in normal hepatocytes, but not in malignant hepatoma cells [3,4]. The regulatory region of the rat *PKM* gene promoter in hepatoma cells consists of multiple GC boxes and a Y box [5]. Whereas both Sp1 and Sp3 bind to the GC boxes, NF-Y binds to the Y box [6]. The overexpression of the dominant negative form of NF-YA decreased transcription from the rat *PKM* gene promoter [6]. However, electrophoretic mobility shift assays using nuclear extracts from normal liver and hepatoma cells revealed that the binding activity of NF-Y to the regulatory element of the *PKM* gene promoter is unchanged between them. Therefore, modification of NF-Y subunits or an interacting partner of the subunits, particularly NF-YA, are important for the biological role of NF-Y. Indeed, we previously reported that the physical interactions between Sp1/Sp3 and NF-YA are critical for functional synergism of the *PKM* gene distal promoter activity [6]. To analyse the molecular mechanism of transcriptional control by NF-Y, we examined the issue of whether the activation domain (AD) of NF-YA interacts with either a known or a novel transcription factor. We previously reported the detection of zinc-fingers and homeoboxes (ZHX) 1 and serum response factor as NF-YA-interacting proteins [7].

ZHX1 consists of 873 amino acid residues and contains two Cys_2-His_2-type zinc-finger (Znf) motifs and five homeodomains (HDs) and belongs to the Znf class of the homeobox protein superfamily [8–11]. The amino acid sequence between 272 and 564 that contains the HD1–HD2 region of human ZHX1 is required for an interaction with the N-terminal glutamine-rich AD of NF-YA [7]. Northern blot analysis revealed that *ZHX1* transcripts were expressed ubiquitously [8–10]. The human *ZHX1* gene is located on chromosome 8q, between markers CHLC.GATA50B06 and CHLC.GATA7G07 [9]. Recently, we also reported that ZHX1 functions as a transcriptional repressor and is localized in the nuclei [12].

In the present study, to determine the biological role of ZHX1, we examined the issue of whether ZHX1 interacts with protein(s)

Abbreviations used: NF-Y, nuclear factor-Y; PKM, pyruvate kinase M; AD, activation domain; ZHX, zinc-fingers and homeoboxes; Znf, zinc finger; HD, homeodomain; DBD, DNA-binding domain; RACE, rapid amplification of cDNA ends; GST, glutathione S-transferase; GFP, green fluorescent protein; ATF, activating transcription factor; ATF-IP, ATF-interacting protein; NLS, nuclear-localization signal; P/CAF, p300/cAMP response element-binding protein-binding protein-associated factor.

[1] To whom correspondence should be addressed (e-mail kazuya@fmsrsa.fukui-med.ac.jp).

The nucleotide sequence of pAD-G58 and the entire coding sequence of human ZHX3 cDNA have been submitted to the DNA Data Bank of Japan under accession numbers AB081947 and AB081948, respectively.

other than NF-YA and regulates gene transcription. Using a yeast two-hybrid system, we conducted a search for ZHX1-interacting proteins in rat liver and ovarian granulosa cell cDNA libraries. Here we report on interactions with BS69 co-repressor, ataxia-related proteins, a leukemia gene, some transcription factors, including ZHX1, and unknown proteins. We mainly report on the cloning of a novel protein, ZHX3, that contains two Znf motifs and five HDs, like ZHX1, and belongs to the ZHX family with ZHX1, and on the detailed characterization of ZHX3 as a nuclear transcriptional repressor.

EXPERIMENTAL

Materials

The yeast two-hybrid system, pDsRed1-C1, X-α-gal, human testis marathon-ready cDNA, Advantage 2 PCR kit, human Multiple Tissue Northern Blot and Blot II, ExpressHyb hybridization solution and pEGFP-C1 were purchased from Clontech (Palo Alto, CA, U.S.A.). The pGEX-4T-2, pGEX-5X-1, [α-^{32}P]dCTP (111 TBq/mmol), ECL Plus Western blotting reagent pack, glutathione–Sepharose 4B and [^{35}S]methionine (37 TBq/mmol) were purchased from Amersham Biosciences (Cleveland, OH, U.S.A.). HEK-293 cells, a human embryonic kidney cell line, were purchased from the American Type Culture Collection (Manassas, VA, U.S.A.). Trizol reagent, Superscript II, pcDNA3.1His-C plasmid and Lipofectamine Plus were purchased from Invitrogen (Groningen, Netherlands). ExTaq DNA polymerase, pT7Blue-T 2 vector and BcaBest DNA-labelling kit were obtained from TaKaRa Biomedicals (Kyoto, Japan). pGEM-T Easy vector, T7 TNT Quick-coupled transcription/translation system, pGL3-Control, pRL-CMV and dual-luciferase assay system were purchased from Promega (Madison, WI, U.S.A.). The Big Dye terminator FS cycle sequencing kit was purchased from Applied Biosystems Japan (Tokyo, Japan). The pCMV-Tag2B plasmid and TOPP3 cells were obtained from Stratagene (La Jolla, CA, U.S.A.). The penta-His antibody and Qiagen plasmid kit were purchased from Qiagen (Hilden, Germany). The FLAG-tagged protein immunoprecipitation kit and anti-FLAG antibody (F7425) were purchased from Sigma (St Louis, MO, U.S.A.). The anti-glutathione S-transferase (GST) antibody (SC-459) was purchased from Santa Cruz Biotechnology (Santa Cruz, CA, U.S.A.). The Immobilon-P PVDF membrane was purchased from Millipore (Bedford, MA, U.S.A.).

Oligonucleotides

The following oligonucleotides were used in this study. S-DsRed1C1-HindIII, 5′-AGCTTCCCGAATTCTGCAG-3′; As-DsRed1C1-SalI, 5′-TCGACTGCAGAATTCGGGA-3′; S-hZHX3-ApaI2, 5′-GTGGCAGACACAGGCAGTG-3′; As-hZHX3-STOP4, 5′-GGCCGGATCCCAGACTGGCCAGTCC-3′; S-hZHX3-NcoI, 5′-CCTGAGCAGCATTCCAACG-3′; As-hZHX3-BsmBI2, 5′-CTTCTTGGTCTCCTCAGCATTCAC-3′; S-hZHX3-Met, 5′-GTGATTGTCACCATGGCCAG-3′; As-hZHX3-NcoI, 5′-GAAGGAGTTCTTCAGGAAGC-3′; S-hZHX3-HD1, 5′-CCGGGAATTCCTGAGCAGCATTCCAAC-GTA-3′; As-hZHX3-HD2, 5′-CCGGGGATCCAGCCCTTCA-AGTTCCGGC-3′; As-hZHX3-1506, 5′-CCGGGGATCCAGA-TTTCTTATTTTTGTAGATGC-3′; S-hZHX3-1090, 5′-CCGG-GAATTCTCCCCTGAGGAGATTGAGG-3′; S-hZHX3-HD2, 5′-CCGGGAATTCTACAAAAATAAGAAATCTCATGAAC-3′; As-hZHX3-HD1, 5′-CCGGGGATCCGGACCAGCTGATCCC-CTG-3′; S-hZHX3N, 5′-GTGGGCTGAGGCACAGACTG-3′; As-hZHX3N, 5′-CCAATCATGAAGATAATGAAAGGC-3′; GBKT7MCS1, 5′-AATTCCCGGG-3′; GBKT7MCS2, 5′-GATCCCGGG-3′; S-GBKT7-NdeI, 5′-TATGGAATTCGC-3′; As-GBKT7-NcoI, 5′-CATGGCGAATTCCA-3′; As-hZHX3-HD1-Eco, 5′-CCGGGAATTCGGACCAGCTGATCCCCTG-3′; S-hZHX3-Met3, 5′-CCGGGAATTCATGGCCAGCAAGAGG-AAATC-3′; As-hZHX3-909, 5′-CCGGGGATCCCAGGGGG-ATCATCACTTTG-3′; As-hZHX3-435, 5′-CCGGGGATCC-TGGCTTGGCCACGTTCCAC-3′; S-hZHX3-436, 5′-CCGG-GAATTCGACAATCATGTGGTTGTGG-3′; As-hZHX3-321, 5′-CCGGGGATCCTGGGTCTTTATTAAAGTCTGTG-3′; S-hZHX3-322, 5′-CCGGGAATTCACCTTTGTATGCAGTGGG-TG-3′; S-hZHX3-1663, 5′-CCGGGAATTCTCCAGAGCGATG-ATACCTG-3′; As-hZHX3-BsmBI-2, 5′-CTTCTTGGTCTCCT-CAGCATTCAC-3′; HisCMCS1, 5′-CAGGGATCCAGTGTGGT-GG-3′; and HisCMCS2, 5′-AATTCCACCACACTGGATCCC-TGGTAC-3′.

Plasmid construction

The pACT2B1 plasmid has been described previously [7]. pAD-G23, a clone isolated from the library screen, was digested with *Eco*RI/*Xho*I or *Sfi*I/*Bgl*II and each fragment was subcloned into the *Eco*RI/*Xho*I sites of the pGEX-4T-2 vector or *Sfi*I/*Bam*HI sites of the pGBKT7 vector to obtain pGST-G23 and pDBD-G23, respectively. A 250-bp *Eco*RI/*Hin*dIII fragment of pAD-G23 was subcloned into the *Eco*RI/*Hin*dIII sites of the pDsRed1-C1 to produce pDsRed-revereseG23 (HD1). The S-DsRed1C1-HindIII and the As-DsRed1C1-SalI oligonucleotides were then annealed, phosphorylated and inserted into the *Hin*dIII/*Sal*I sites of the pDsRed1-C1 to obtain pDsRed1-C1E1. An *Eco*RI/*Bgl*II fragment of the pDsRed-revereseG23 (HD1) was subcloned into the *Eco*RI/*Bam*HI sites of the pDsRed1-C1E1 to produce pDsRed-rZHX3 (HD1). The *Eco*RI/*Xho*I fragment of the resultant plasmid was subcloned into the *Eco*RI/*Xho*I sites of the pACT2 to produce pAD-ZHX3 (242-488).

pBSII-KIAA0395 was a gift from Dr Takahiro Nagase (Kazusa DNA Research Institute, Chiba, Japan). A 1.2-kb *Sal*I/*Apa*I fragment of the plasmid was subcloned into the *Sal*I/*Apa*I sites of the pDsRed1-C1E1 to produce pDsRed-ZHX3 (HD2–5). The *Bgl*II/*Bam*HI fragment of the resultant was subcloned into the *Bam*HI site of pACT2B1 to obtain pAD-ZHX3 (498-903).

The pAD-ZHX1 (142-873) (previously referred to as pACT2-#111), pAD-ZHX1 (272-873), pAD-ZHX1 (565-873), pAD-ZHX1 (272-564), pAD-ZHX1 (272-432), pAD-ZHX1 (430-564), pAD-ZHX1 (345-463), pDBD, pYA1-269, pYA1-140, pYA1-112, pYA141-269, pYA172-269 and pYA205-269 have been described previously [pAD-ZHX1 constructs and pDBD were previously referred to as the pZHX1-constructs and pGBT9 (N/R/N), respectively] [7,9].

Total RNA from HEK-293 cells was prepared using the Trizol reagent according to the manufacturer's protocol. Reverse transcriptase PCRs were performed as described previously with minor modification [9]. PCR conditions were described previously except for the use of the ExTaq DNA polymerase [9]. Combinations of S-hZHX3-ApaI2 and As-hZHX3-STOP4, S-hZHX3-NcoI and As-hZHX3-BsmBI2, S-hZHX3-Met and As-hZHX3-NcoI, S-hZHX3-HD1 and As-hZHX3-HD2, S-hZHX3-HD1 and As-hZHX3-1506, S-hZHX3-1090 and As-hZHX3-HD2, S-hZHX3-HD2 and As-hZHX3-HD2, S-hZHX3-HD1 and As-hZHX3-HD1, and S-hZHX3N and As-hZHX3N, were used as primers. These products were subcloned into the pGEM-T Easy vector to give pGEM-T Easy ZHX3 (ApaI/STOP), pGEM-T Easy ZHX3 (NcoI/BsmBI), pGEM-T

Easy ZHX3 (Met/NcoI), pGEM-T Easy ZHX3 (HD1-2), pGEM-T Easy ZHX3 (HD1-1506), pGEM-T Easy ZHX3 (1090-HD2), pGEM-T Easy ZHX3 (HD2), pGEM-T Easy ZHX3 (HD1) and pGEM-T Easy ZHX3N, respectively.

GBKT7MCS1 and GBKT7MCS2 oligonucleotides were annealed, phosphorylated and subcloned into the *Eco*RI/*Bam*HI sites of pGBKT7 to give pGBKT7B1. The *Apa*I/*Bam*HI fragment of the pGEM-T Easy ZHX3 (ApaI/STOP) was subcloned into the *Apa*I/*Bam*HI sites of the pDsRed-ZHX3 (HD2-5) to give pDsRed-ZHX3 (HD2-STOP). The *Eco*RI/*Bsm*BI fragment of pGEM-T Easy ZHX3 (NcoI/BsmBI) was subcloned into the *Eco*RI/*Bsm*BI sites of pDsRed-ZHX3 (HD2-STOP) to give pDsRed-ZHX3 (NcoI-STOP). S-GBKT7-NdeI and As-GBKT7-NcoI oligonucleotides were annealed, phosphorylated and inserted into the *Nde*I/*Nco*I sites of pGBKT7B1 to give pGBKT7NEN. A 2-kb *Nco*I/*Bam*HI fragment of the pDsRed-ZHX3 (NcoI-STOP) was subcloned into the *Nco*I/*Bam*HI sites of the pGBKT7NEN to produce pGBKT7-ZHX3 (NcoI-STOP). pGEM-T Easy ZHX3 (Met/NcoI) was digested with *Nco*I and the 960-bp fragment was subcloned into the *Nco*I site of pGBKT7-ZHX3 (NcoI-STOP) to give pDBD-ZHX3 (1-956). The resultant plasmid was digested with *Bam*HI, blunt-end ligated by the Klenow reaction, and then digested with *Eco*RI. The 2.9-kb fragment was subcloned into the *Eco*RI/*Sma*I sites of the pGEX-5X-1 vector to obtain pGST-ZHX3 (1-956). The *Eco*RI/*Xho*I fragment of the pGST-ZHX3 (1-956) was subcloned into the *Eco*RI/*Xho*I sites of the pACT2B1 to produce pAD-ZHX3 (1-956). PCRs were carried out using the pDBD-ZHX3 (1-956) as a template with the combination of S-hZHX3HD1 and As-hZHX3-HD1-Eco as primers. After digestion with *Eco*RI, the fragment was subcloned into the *Eco*RI site of pACT2B1 to give pAD-ZHX3 (303-364).

A 2.9-kb *Eco*RI/*Xho*I fragment of the pAD-ZHX3 (1-956) was subcloned into the *Eco*RI/*Xho*I sites of the pCMV-Tag2B to obtain pFLAG-ZHX3 (1-956). The pBSII-hZHX1E/X has been described previously [9]. A 3.5-kb *Eco*RI/*Xho*I fragment of the plasmid was subcloned into the *Eco*RI/*Xho*I sites of the pcDNA3.1His-C to give pcDNA3.1His-C-ZHX1EX. A 0.9-kb *Eco*RI fragment of the pGEM-T Easy-ZHX1 (1-271) was subcloned into the *Eco*RI of the resultant plasmid to produce pHis-ZHX1 (1-873).

The pSG424, pSG424B1, 5xGAL4-pGL3 Control and pEGFP-C1E1 plasmids have been described previously [6,13–15]. The 2.9-kb *Eco*RI/*Bam*HI fragment of the pDBD-ZHX3 (1-956) was subcloned into the *Eco*RI/*Bam*HI sites of the pSG424B1 or pEGFP-C1E1 vector to give pGAL4-ZHX3 (1-956) and pGFP-ZHX3 (1-956), respectively. The *Bgl*II/*Bam*HI fragment of the pDsRed-ZHX3 (HD2-5) was subcloned into the *Bam*HI site of pSG424B1 to give pGAL4-ZHX3 (498-903). The *Eco*RI/*Bam*HI fragments of the pGEM-T Easy ZHX3 (HD1-2), pGEM-T Easy ZHX3 (HD1-1506), pGEM-T Easy ZHX3 (1090-HD2) and pGEM-T Easy ZHX3 (HD2) were subcloned into the *Eco*RI/*Bam*HI sites of the pSG424B1 or pEGFP-C1E1 vector to produce pGAL4-ZHX3 (303-555), pGAL4-ZHX3 (303-502), pGFP-ZHX3 (303-555), pGFP-ZHX3 (303-502), pGFP-ZHX3 (364-555) and pGFP-ZHX3 (497-555), respectively. The *Eco*RI/*Bam*HI fragment of the pGEM-T Easy ZHX3 (HD1) was subcloned into the *Eco*RI/*Bam*HI sites of the pSG424B1 vector to obtain pGAL4-ZHX3 (303-364).

PCRs were also carried out using pDBD-ZHX3 (1-956) as a template with the combination of S-hZHX3-Met3 and As-hZHX3-909, S-hZHX3-Met3 and As-hZHX3-435, S-hZHX3-436 and As-hZHX3-909, S-hZHX3-Met3 and As-hZHX3-321, S-hZHX3-322 and As-hZHX3-435, and S-hZHX3-1663 and As-hZHX3-BsmBI-2, as primers, and using the pGFP-ZHX3 (303-555) as a template with the combination of S-hZHX3-1090 and As-hZHX3-1506 as primers. Amplified DNAs were also subcloned into the pGEM-T Easy or pT7Blue-2 T vector to produce pGEM-T Easy ZHX3 (Met/909), pGEM-T Easy ZHX3 (Met/435), pGEM-T Easy ZHX3 (436/909), pT7Blue-2 T ZHX3 (Met/321), pT7Blue-2 T ZHX3 (322/435), pGEM-T Easy ZHX3 (1663/2022) and pGEM-T Easy ZHX3 (1090/1506), respectively. The *Eco*RI/*Bam*HI fragments of these plasmids were subcloned into the *Eco*RI/*Bam*HI sites of the pSG424B1 or pEGFP-C1E1 vector to produce pGAL4-ZHX3 (1-145), pGAL4-ZHX3 (146-303), pGFP-ZHX3 (1-303), pGFP-ZHX3 (1-107), pGFP-ZHX3 (108-145) and pGFP-ZHX3 (146-303), respectively. The *Eco*RI/*Bam*HI fragment of the pGEM-T Easy ZHX3 (1090/1506) was subcloned into the *Eco*RI/*Bam*HI sites of the pSG424B1 to produce pGAL4-ZHX3 (364-502). The *Eco*RI/*Bsm*BI fragment of the pGEM-T Easy ZHX3 (1663/2022) was subcloned into the *Eco*RI/*Bsm*BI sites of the pDsRed-ZHX3 (HD2-STOP) to produce pDsRed-ZHX3 (1663-STOP). The *Eco*RI/*Bam*HI fragment of the resultant plasmid was subcloned into the *Eco*RI/*Bam*HI sites of the pEGFP-C1E1 to produce pGFP-ZHX3 (555-956).

HisCMCS1 and HisCMCS2 oligonucleotides were annealed, phosphorylated and subcloned into the *Kpn*I/*Eco*RI sites of the pcDNA3.1His-C to give the pcDNA3.1His-C2. The pGST-ZHX1 (272-432) was described previously [12]. A 480-bp *Bam*HI fragment of the pGST-ZHX1 (272-432) was subcloned into the *Bam*HI site of the pcDNA3.1His-C2 to produce pCMV-ZHX1 (272-432).

The nucleotide sequences of all inserts were confirmed using a DNA sequencer 3100 (Applied Biosystems).

Library screening

pDBD-ZHX1 (1-873) [previously referred to as pGBKT7-ZHX1 (1-873)], which expresses the entire coding sequence of human ZHX1 fused to the DNA-binding domain (DBD) of yeast transcription factor GAL4, and the construction of rat granulosa cell and liver cDNA libraries were described previously [10,16]. AH109 yeast cells were transformed with the pDBD-ZHX1 (1-873) plasmid. The strain was used as a bait to screen cDNA libraries. A Tris/EDTA/lithium acetate-based high-efficiency transformation method was used for library screening [17]. We plated approx. 1.5×10^7 and 1.1×10^7 independent clones of the liver and granulosa cell cDNA libraries on to histidine-, tryptophan-, leucine- and adenine-free synthetic dextrose plates supplemented with 4 mM 3-aminotriazole and X-α-gal, respectively. Thus 33 and 109 positive clones were obtained from the primary transformants, respectively. The yeast strain SFY526, which contains a quantifiable *lacZ* reporter, and either the pGBKT7 or pDBD-ZHX1 (1-873) plasmids, was transformed with plasmids isolated from positive clones in primary screening of the parent vector, pACT2. In the second screening, 16 and 25 clones from liver and granulosa cell cDNA libraries, respectively, specifically exhibited reproducible high β-galactosidase activity. Quantitative β-galactosidase assays, using *o*-nitrophenyl-β-D-galactoside, were carried out on permeabilized cells, as described previously [7,9,18]. Nucleotide sequences from each positive clone were compared with those entered in the GenBank database using the BLAST sequence search and comparison program.

Rapid amplification of cDNA ends (RACE)

To obtain the 5′ end of the human ZHX3 cDNA, we employed a 5′-RACE method using human testis marathon-ready cDNA and

the Advantage 2 PCR kit. Two gene-specific primers, hZHX3-5RACE-As1, 5′-GGCATCTTGCAACACCACAGTCTTC-3′, and hZHX3-5RACE-As2, 5′-CATGCATGGTGTGGTGGATTT-CCTC-3′, were used. The 5′-RACE procedure was carried out according to the manufacturer's recommended protocol. Amplified DNA fragments were subcloned into the pGEM-T Easy vector and their nucleotide sequences determined.

Poly(A)$^+$ RNA blot analysis

A 0.6-kb *Eco*R I fragment of the human ZHX3 cDNA that was isolated from the pGEM-T Easy hZHX3N plasmid and a 2.0-kb human β-actin fragment were used as the probes. Probe DNAs were labelled with [α-^{32}P]dCTP using the BcaBest DNA labelling kit. Human Multiple Tissue Northern Blot and Blot II were hybridized with each ^{32}P-labelled probe. The ExpressHyb hybridization solution was used for prehybridization and hybridization. Prehybridization, hybridization and washing procedures were performed according to the protocol provided by the supplier.

Yeast two-hybrid system and liquid β-galactosidase assays

To analyse the heterodimerization domain of ZHX1 with ZHX3, SFY526 yeast strains harbouring pDBD or pDBD-G23 were transformed with various truncated forms of ZHX1 fused to the GAL4 AD, or pACT2. To map the heterodimerization domain of ZHX3 with ZHX1 or the homodimerization domain of ZHX3, SFY526 yeast strains harbouring the pDBD, pDBD-ZHX1 (1-873), or pDBD-G23 were transformed with various truncated forms of ZHX3 fused to the GAL4 AD, or pACT2. In order to examine the interaction domain of ZHX3 with NF-YA, SFY526 yeast strains harbouring pDBD or pYA1-269 were transformed with various truncated forms of ZHX3 fused to the GAL4 AD. For mapping the interacting domain of NF-YA with ZHX3, a SFY526 yeast strain harbouring pAD-ZHX3 (242-488) was transformed with various truncated forms of NF-YA fused to the GAL4 DBD. These β-galactosidase activities were determined as described previously [7,9,10].

GST pull-down assays

The pGST-ZHX1 (1-873) plasmids have been described previously [10]. TOPP3 cells were transformed with pGEX-5X-1, pGST-ZHX1 (1-873), pGST-G23 or the pGST-ZHX3 (1-956) fusion-protein expression plasmid. The preparation of the GST fusion protein, ^{35}S-labelling of *in vitro*-translated ZHX1 and pull-down analysis have been described previously [9,10]. The pDBD-ZHX3 (1-956) plasmid was employed for the preparation of *in vitro*-translated ^{35}S-labelled ZHX3. Finally, the beads were resuspended in an equal volume of 2 × SDS sample buffer and each supernatant was loaded on to an SDS/PAGE gel (10 %), along with a prestained molecular-mass marker. The gel was dried and exposed to a FUJIX imaging plate (Kanagawa, Japan). Interaction signals were detected using the FUJIX BAS-2000 image analysing system. The relative purity and amounts of each fusion protein were determined by gel-staining with Coomassie Brilliant Blue R-250.

Cell culture and DNA transfections

HEK-293 cells were cultured in Dulbecco's modified Eagle's medium supplemented with 10 % fetal bovine serum at 37 °C in a 5 % CO_2 incubator.

DNA transfections were carried out using the Lipofectamine Plus reagents. All plasmids used for the transfection were prepared using a Qiagen plasmid kit, followed by CsCl gradient ultracentrifugation. For co-immunoprecipitation assays, 6×10^5 cells were plated in a 6-cm-diameter dish. After 24 h, 1 μg of both the pHis-ZHX1 (1-873) and pFLAG-ZHX3 (1-956) plasmids was transfected into the cells. Cell were harvested at 48 h after transfection, followed by the immunoprecipitation assay. For determination of transcriptional activity and analysis of subcellular localization, cells (5×10^4/well) were inoculated in a 24-well plate on the day prior to transfection. The 5xGAL4-pGL3 Control has been described previously [14]. 5xGAL4-pGL3 Control or pGL3-Control was employed as the reporter plasmid. For the determination of transcriptional activity of ZHX3, 100 ng of a reporter plasmid, 2 ng of the pRL-CMV and the indicated amount of GAL4 DBD–ZHX3 fusion-protein expression plasmid were transfected. The total amount of plasmid (152 ng) was adjusted by the addition of the pSG424, if required. For the analysis of effects of heterodimerization of ZHX3 with ZHX1 on the transcriptional activity of ZHX3, 100 ng of a reporter plasmid, 2 ng of the pRL-CMV, 50 ng of GAL4 DBD fusion-protein expression plasmids, and the indicated amount of the expression plasmid for the dimerization domain of the human ZHX1, pCMV-ZHX1 (272-432), were transfected. The total amount of plasmid (202 ng) was adjusted by the addition of the pcDNA3.1His-C2, if necessary. For observation of the green fluorescent protein (GFP) fusion protein, 300 ng of the indicated GFP plasmid was transfected. Then, 3 h after transfection, the medium was changed. After 48 h the cells were subjected to luciferase assays or observed with a laser microscope (Olympus) [15]. Firefly and sea pansy luciferase assays were performed according to the manufacturer's recommended protocol (Promega). Luciferase activities were determined by a Berthold Lumat model LB 9501 (Wildbad, Germany). Firefly luciferase activities (relative light units) were normalized by sea pansy luciferase activities.

Co-immunoprecipitation assays

The FLAG-tagged ZHX3 was affinity-purified from lysates of HEK-293 cells that were transfected with both the pFLAG-ZHX3 (1-956) and pHis-ZHX1 (1-873) plasmids using the FLAG protein immunoprecipitation kit. Procedures were according to the manufacturer's recommended protocol. The FLAG-tagged ZHX3 was eluted with 3 × FLAG peptide, subjected to SDS/PAGE (10 % gel), and blotted on to an Immobilon-P PVDF membrane. The FLAG-tagged ZHX3 and His-tagged ZHX1 proteins were visualized using anti-FLAG or anti-penta-His antibody and the ECL Plus Western blotting reagent pack.

RESULTS

Screening of ZHX1-interacting proteins

To analyse the molecular mechanism of transcriptional repression by ZHX1, we examined the issue of whether the human ZHX1 interacts with either a known or a novel transcription factor. An entire coding sequence of the human ZHX1 was fused to the GAL4 DBD and this chimaeric protein was employed as the bait to screen rat liver and granulosa cell cDNA libraries using the yeast two-hybrid system. Approx. 1.5×10^7 and 1.1×10^7 independent clones of each library were screened, and 16 and 25 clones showed reproducible His$^+$, Ade$^+$ and α-gal-positive properties, respectively. We isolated plasmids that encode the GAL4 AD fusion protein from these clones. After determination of their nucleotide sequences, they were compared with the

Table 1 The ZHX1-interacting proteins

Protein	Number of clones
BS69 co-repressor	9
Nuclear protein, ataxia-telangiectasia-like protein	5
Androgen-induced aldose reductase	3
ATF-IP	2
Spinocerebellar ataxia type I	2
Zyxin	2
Elf-1	1
Eleven-nineteen lysine-rich leukemia gene	1
ZHX1	8
Unknown	8

GenBank database using the BLAST search program. As shown in Table 1, the BS69 co-repressor, nuclear protein, ataxia-telangiectasia-like protein, androgen-induced aldose reductase, activating transcription factor (ATF)-interacting protein (ATF-IP), spinocerebellar ataxia type I, zyxin, Elf-1, eleven-nineteen lysine-rich leukemia gene and ZHX1 were cloned as known proteins [10,19–26]. Eight clones encoded unknown proteins. Interestingly, three clones, G23, G58 and L26, encoded both Znf and HD motifs. A detailed nucleotide sequence analysis showed that the nucleotide sequence of G23 was included in that of G58, and that the nucleotide sequence exhibited a similarity to that of partially cloned human KIAA0395 cDNA. We focused on the analysis of these clones in this study. The L26 clone, differing from the KIAA0395, has been denoted ZHX2 (H. Kawata and K. Yamada, unpublished work) and will be reported on in the future.

In order to isolate the 5′-non-coding sequence and the remaining coding region of the human KIAA0395 cDNA, we then employed a 5′-RACE method. Using combinations of gene-specific primers and adaptor primers, a cDNA fragment was obtained by PCR using human testis marathon cDNA as a template. Finally, the size of the full-length cDNA was determined to be 9302 bp. The full-length cDNA has an open reading frame of 956 amino acid residues. Nucleotide and amino acid sequences were identical to a putative protein TIX1 (triple homeobox 1; accession nos. XP029734 and XM029734). However, very interestingly, the deduced amino acid sequence of the protein contains two Cys_2-His_2-type Znf motifs and five HDs as well as ZHX1 (Figure 1).

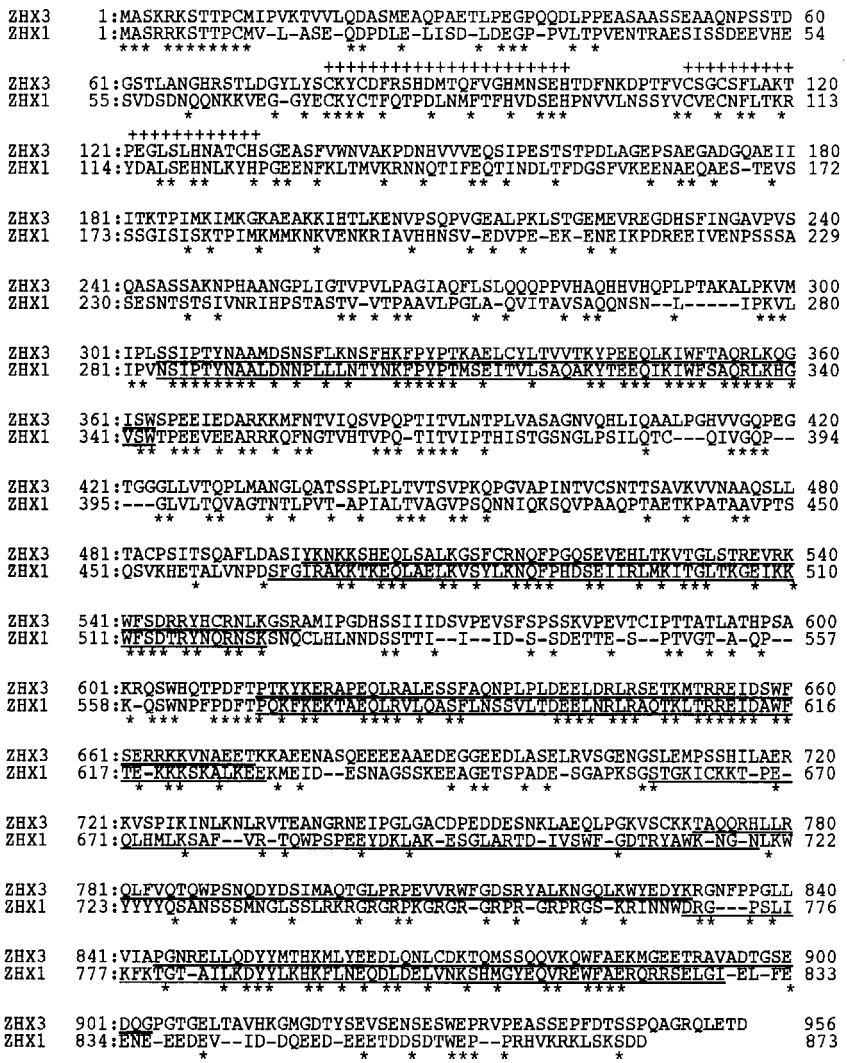

Figure 1 A comparison of deduced amino acid sequences of human ZHX3 with human ZHX1

The two Znf motifs and five HDs are indicated by plus signs and underlines, respectively. The asterisks indicate amino acid identity. The dashes indicate a gap when no corresponding amino acid sequence exists in the other protein. The deduced amino acid sequences of clones G58 and G23, and KIAA0395, correspond to human ZHX3 residues 114–642, 242–615 and 495–956, respectively.

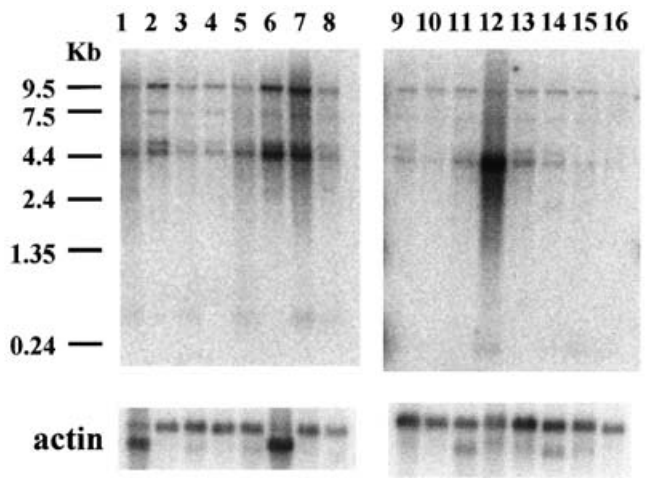

Figure 2 Tissue distribution of human ZHX3 mRNA

Human Multiple Tissue Northern Blot and Blot II were hybridized with ^{32}P-labelled human ZHX3 (upper panels) or human β-actin cDNA (lower panels). Prehybridization and hybridization procedures are described in the Experimental section. Each lane contains 2 μg of poly(A)$^+$ RNA isolated from indicated tissues. Size markers are shown on the left in kb. Lane 1, heart; lane 2, brain; lane 3, placenta; lane 4, lung; lane 5, liver; lane 6, skeletal muscle; lane 7, kidney; lane 8, pancreas; lane 9, spleen; lane 10, thymus; lane 11, prostate; lane 12, testis; lane 13, ovary; lane 14, small intestine; lane 15, colon; lane 16, leucocyte.

Hereafter, we refer to the protein as ZHX3 (the name ZHX3 has been submitted to the HUGO Nomenclature Committee with the name zinc-fingers and homeoboxes 3). The human ZHX3 protein has a predicted molecular mass of 104.7 kDa and a pI of 5.68. Whereas pAD-G58 and pAD-G23 encoded amino acid sequence between 114 and 642 and between 242 and 615 of the ZHX3, respectively, KIAA0395 encoded amino acid sequence between 498 and 956 of the human ZHX3. A glutamic-acid-rich region that may act as a transcription regulatory domain existed in the amino acid sequence between 670 and 710 and no putative nuclear-localization signals (NLSs) exist. The similarity in nucleotide sequences in the coding region and amino acid sequences between ZHX3 and ZHX1 were 46.9 and 34.4 %, respectively (Figure 1).

We then determined the tissue distribution of human ZHX3 mRNA by Northern blot analysis. As shown in Figure 2, human ZHX3 mRNA was detected as multiple bands, 9.4, 7.3, 5.0 and 4.6 kb in length. Since the size of our cloned insert was 9302 bp, it is almost identical with the full-length transcript. These transcripts were observed in all the tissues examined, although the intensity varied among tissues. This indicates that human ZHX3 mRNA is expressed ubiquitously.

Mapping of the minimal hetero-dimerization domain between ZHX1 and ZHX3

We examined the issue of which domain of ZHX1 is required for interaction with ZHX3. A yeast strain SFY526 was transformed with the pDBD, which expresses GAL4 DBD alone, or pDBD-G23, which encodes amino acid residues 242–615 of the ZHX3 fused to GAL4 DBD. The two yeast strains were used as the reporter yeasts. pACT2, which expresses GAL4 AD alone or some plasmids, which encode various truncated forms of ZHX1 fused to the GAL4 AD, were employed as the prey plasmids. When a reporter yeast harbouring the pDBD was transformed with these prey plasmids, they showed low β-galactosidase activities (results not shown). In addition, when a reporter yeast harbouring the pDBD-G23 was transformed with the pACT2, pAD-ZHX1 (565-873), pAD-ZHX1 (430-564) or pAD-ZHX1 (345-463), these yeasts also showed low β-galactosidase activities (Figure 3A). In contrast, when the yeast was transformed with the pAD-ZHX1 (142-873), pAD-ZHX1 (272-873), pAD-ZHX1 (272-564)

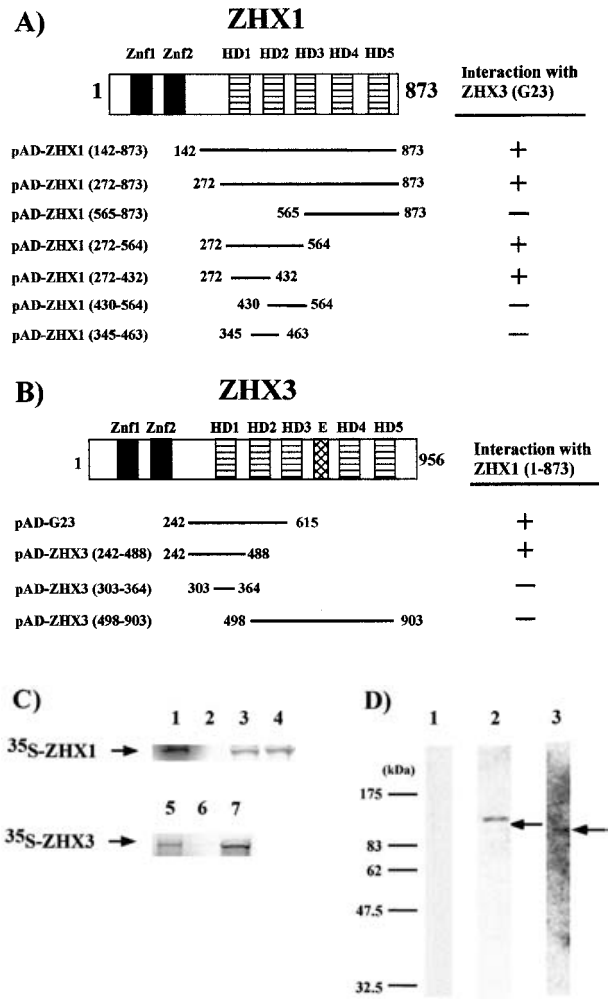

Figure 3 Identification of the minimal heterodimerization domain between ZHX1 and ZHX3 using the yeast two-hybrid system, GST pull-down assays and co-immunoprecipitation assay

(**A**) A schematic representation of human ZHX1 and the GAL4 AD–ZHX1 fusion constructs is depicted on the left. The + and − symbols indicate increased and unchanged levels of β-galactosidase activity, respectively, compared with a yeast harbouring a combination of pDBD-G23, expressing amino acids 242–488 of human ZHX3 fused to the GAL4 DBD, and pACT2. (**B**) A schematic representation of human ZHX3 and the GAL4 AD–ZHX3 fusion constructs is depicted on the left. E indicates a glutamic-acid-rich region. + and − indicate increased and unchanged levels of β-galactosidase activity, respectively, compared with a yeast harbouring a combination of pDBD-ZHX1 (1-873), expressing the entire coding region of human ZHX1 fused to the GAL4 DBD, and pACT2. (**C**) *In vitro* heterodimerization between ZHX1 and ZHX3 using GST pull-down assays. *In vitro*-translated, ^{35}S-labelled full-length human ZHX1 or ZHX3 was incubated with Sepharose beads containing bound GST alone (lanes 2 and 6) or amino acids 242–615 of ZHX3 (lane 3), or the entire coding sequences of human ZHX3 (lane 4) or ZHX1 (lane 7) protein fused to GST. The beads were washed thoroughly and the bound protein was eluted and analysed by SDS/PAGE (10 % gel). Interaction signals were detected by an autoradiography. Lanes 1 and 5, 10 % of the protein added to the reactions shown in the other lanes were loaded. (**D**) Co-immunoprecipitation assays. The FLAG-tagged ZHX3 was affinity-purified from lysates of HEK-293 cells that were transfected with both the pFLAG-ZHX3 (1-956) and pHis-ZHX1 (1-873) plasmids using anti-FLAG-antibody-immobilized column. The eluate was then subjected to SDS/PAGE (10 % gel) and electroblotted on to PVDF membrane. The FLAG-tagged ZHX3 and His-tagged ZHX1 proteins were visualized using anti-FLAG or anti-penta-His antibodies and the ECL Plus Western blotting reagent pack. Lane 1, anti-GST antibody; lane 2, anti-FLAG antibody; lane 3, anti-penta-His antibody.

or pAD-ZHX1 (272-432), high β-galactosidase activities were observed. pAD-ZHX1 (272-432) encodes amino acid residues between 272 and 432 of ZHX1.

We then determined the issue of which domain of ZHX3 is required for an interaction with ZHX1. Yeast strain SFY526 was transformed with pDBD-ZHX1 (1-873), which encodes an entire coding sequence of the ZHX1 fused to GAL4 DBD, or pDBD. The two yeast strains were used as the reporter yeasts. The pACT2 or some plasmids encoding various truncated forms of ZHX3 fused to the GAL4 AD were employed as prey plasmids (Figure 3B). When a reporter yeast harbouring the pDBD was transformed with these prey plasmids, they showed low β-galactosidase activities (results not shown). These yeasts showed high β-galactosidase activities only when a reporter yeast harbouring pDBD-ZHX1 (1-873) was transformed with pAD-G23 or pAD-ZHX3 (242-488). pAD-ZHX3 (242-488) encodes the amino acid residues between 242 and 488 of ZHX3.

We also carried out *in vitro* GST pull-down assays to verify the specific interaction between ZHX1 and ZHX3. We employed four plasmids, pGEX-5X-1, which expresses GST alone, pGST-G23, which encodes the amino acids 242–615 of human ZHX3 fused to GST, pGST-ZHX3 (1-956), which expresses the entire coding region of human ZHX3 protein fused to GST, and pGST-ZHX1 (1-873), which expresses the entire coding region of human ZHX1 protein fused to GST. These proteins were expressed in *Escherichia coli* and immobilized on to glutathione–Sepharose beads. The *in vitro*-translated, ^{35}S-labelled full-length of human ZHX1 was found to bind to GST–G23 and GST–ZHX3 (1-956) but not to GST alone (Figure 3C). In addition, the *in vitro*-translated, ^{35}S-labelled full-length human ZHX3 was found to bind to GST–ZHX1 (1-873) but not to GST alone (Figure 3C). In contrast, an unprogrammed reticulocyte lysate failed to bind to any of the proteins (results not shown).

To detect an interaction of ZHX1 with ZHX3 in mammalian cells, both His-tagged ZHX1 and FLAG-tagged ZHX3 proteins are expressed in HEK-293 cells. Lysates of the cells were subjected to affinity purification of FLAG protein using anti-FLAG antibody-immobilized agarose column. After bound proteins were eluted with the 3 × FLAG peptide from the column, these were subjected to SDS/PAGE, then followed by Western blot analysis using anti-GST, anti-FLAG or anti-His antibodies. As shown in Figure 3(D), both FLAG-tagged ZHX3 and His-tagged ZHX1 proteins but not GST protein were detected. In contrast, no bands were observed in lysates of untreated HEK-293 cells (results not shown). These results indicate that ZHX1 is able to form a heterodimer with ZHX3 both *in vivo* and *in vitro*.

Mapping of the minimal homodimerization domain of ZHX3

Since ZHX1 forms a homodimer [10], we then investigated formation of a homodimer for ZHX3 using the yeast two-hybrid system. Two SFY526 yeast strains harbouring pDBD or pDBD-G23 were used as the reporter yeasts. We prepared various prey plasmids, pACT2, pAD-G23, pAD-ZHX3 (242-488), pAD-ZHX3 (303-364) and pAD-ZHX3 (498-903). These plasmids were transformed into the reporter yeasts and β-galactosidase activity was determined in each case (Figure 4A). When the reporter yeast harbouring pDBD was transformed with the plasmids, they showed very low β-galactosidase activities (results not shown). In addition, when a reporter yeast harbouring pDBD-G23 was transformed with pACT2, pAD-ZHX3 (303-364) and pAD-ZHX3 (498-903), very low β-galactosidase activity was also detected. In contrast, the yeast transformed with pAD-G23 or pAD-ZHX3 (242-488) expressed high β-galactosidase activities. These results indicate that ZHX3 is able to form a homodimer via the region between residues 242 and 488.

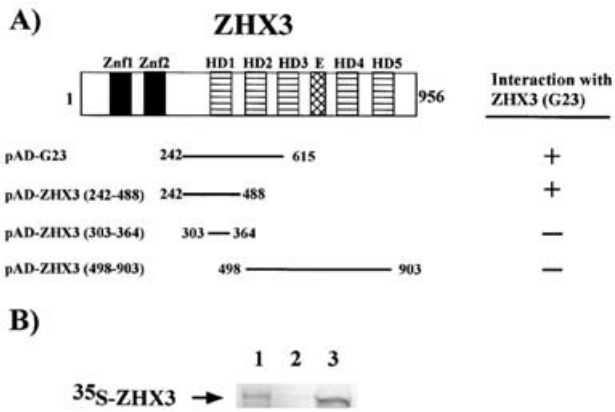

Figure 4 Identification of the minimal homodimerization domain of ZHX3 using a yeast two-hybrid system or GST pull-down assay

(**A**) Human ZHX3 and the GAL4 AD–ZHX3 fusion constructs are depicted on the left. E indicates a glutamic-acid-rich region. + and − symbols indicate the same as described for Figure 3(A). (**B**) *In vitro* homodimerization of ZHX3 using the GST pull-down assays. *In vitro*-translated, ^{35}S-labelled full-length human ZHX3 was incubated with Sepharose beads containing bound GST alone (lane 2) or the entire coding sequence of human ZHX3 protein fused to GST (lane 3). Procedures were the same as those described for Figure 3(C). Lane 1, 10 % of the protein added to the reactions shown in the other lanes was loaded.

We then carried out *in vitro* GST pull-down assays to verify the homodimerization of ZHX3. We employed two plasmids, pGEX-5X-1 and pGST-ZHX3 (1-956). These proteins were expressed in *E. coli* and immobilized on to glutathione–Sepharose beads. The *in vitro*-translated, ^{35}S-labelled full-length human ZHX3 was found to bind to GST-ZHX3 (1-956) but not to GST alone (Figure 4B). In contrast, an unprogrammed reticulocyte lysate failed to bind to any of the proteins (results not shown). These results indicate that ZHX3 is able to form a homodimer *in vivo* and *in vitro*.

ZHX3 also interacts with the AD of the NF-YA

Human ZHX1 was originally cloned as a protein that interacts with NF-YA [9]. We also examined the interaction of ZHX3 with NF-YA using the yeast two-hybrid system. We used two reporter-yeast strains, which are transformed with pDBD or pYA1-269. pYA1-269 expresses the AD of the NF-YA fused to the GAL4 DBD. pACT2, pAD-ZHX3 (1-956), pAD-G23, pAD-ZHX3 (242-488), pAD-ZHX3 (303-364) and pAD-ZHX3 (498-903) were transformed into the reporter yeast strains and their β-galactosidase activities determined. When a reporter yeast harbouring the pDBD was transformed with these plasmids, their β-galactosidase activities were found to be quite low (results not shown). As shown in Figure 5(A), when a reporter yeast harbouring pYA1-269 was transformed with pACT2, pAD-ZHX3 (303-364) or pAD-ZHX3 (498-903), their β-galactosidase activities were also low. However, when the yeast was transformed with pAD-ZHX3 (1-956), pAD-G23 or pAD-ZHX3 (242-488), high levels of β-galactosidase activity were detected. These results indicate that ZHX3 interacts with the AD of the NF-YA, and that the amino acid sequence between residues 242 and 488 is essential for this interaction.

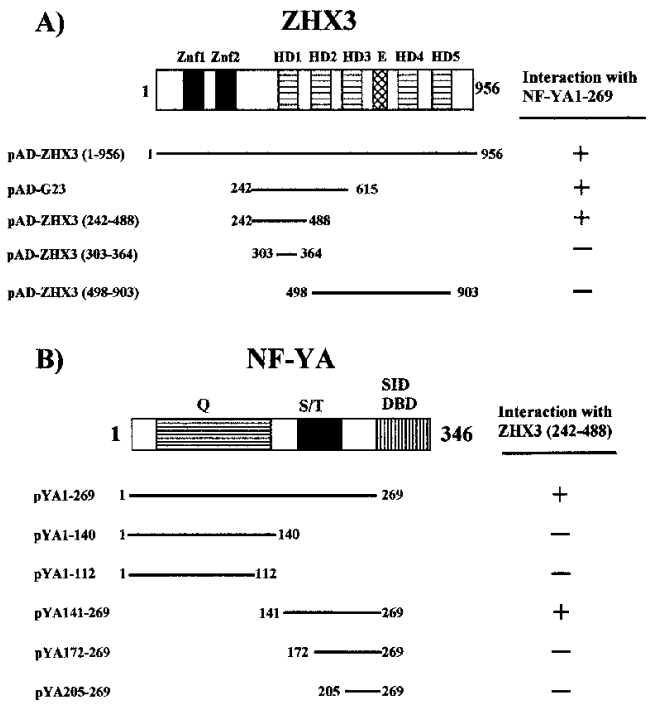

Figure 5 Interaction domain mapping between NF-YA and ZHX3 using the yeast two-hybrid system

(**A**) Human ZHX3 and the GAL4 AD–ZHX3 fusion constructs are depicted on the left. E indicates a glutamic-acid-rich region. + and — indicate increased and unchanged levels of β-galactosidase activity, respectively, compared with a yeast harbouring a combination of pYA1-269, expressing the NF-YA AD fused to the GAL4 DBD, and pACT2. (**B**) Schematic diagram of NF-YA and its deletion mutants fused to the GAL4 DBD are illustrated. Q and S/T indicate glutamine- and serine/threonine-rich regions, respectively. SID indicates the subunit-interaction domain. The + and — symbols indicate increased and unchanged levels of β-galactosidase activity, respectively, compared with a yeast harbouring a combination of pDBD and pAD-ZHX3 (242–488), expressing amino acids 242–488 of human ZHX3 fused to the GAL4 AD.

We next identified the minimal interaction domain of NF-YA with ZHX3 using the yeast two-hybrid system. As shown in Figure 5(B), the AD of NF-YA consists of a glutamine-rich and a serine/threonine-rich domain [1]. The SFY526 yeast strain harbouring pAD-ZHX3 (242-488) was used as a reporter yeast. Various plasmids expressing truncated forms of the NF-YA fused to the GAL4 DBD were transformed in the yeast and their β-galactosidase activities determined. As a result, only yeasts harbouring the pYA1-269 or pYA141-269, both of which contain amino acids 141-269 of NF-YA, showed a high level of β-galactosidase activity. These results indicate that a serine/threonine-rich AD of NF-YA represents the minimal interaction domain with ZHX3.

ZHX3 is a transcriptional repressor

We then determined the transcriptional role of ZHX3 using a mammalian one-hybrid system. The 5xGAL4-pGL3 Control plasmid, in which five copies of the GAL4-binding site had been inserted upstream of the simian virus 40 (SV40) promoter of pGL3-Control, was employed as a reporter plasmid [14]. Two effector plasmids, pSG424, which expresses GAL4 DBD alone, and pGAL4-ZHX3 (1-956), which expresses the entire coding region of human ZHX3 fused to the C-terminus of the GAL4 DBD, were prepared. As shown in Figure 6, when 5xGAL4-pGL3 Control and various amounts of pGAL4-ZHX3 (1-956) were co-transfected into HEK-293 cells, the luciferase

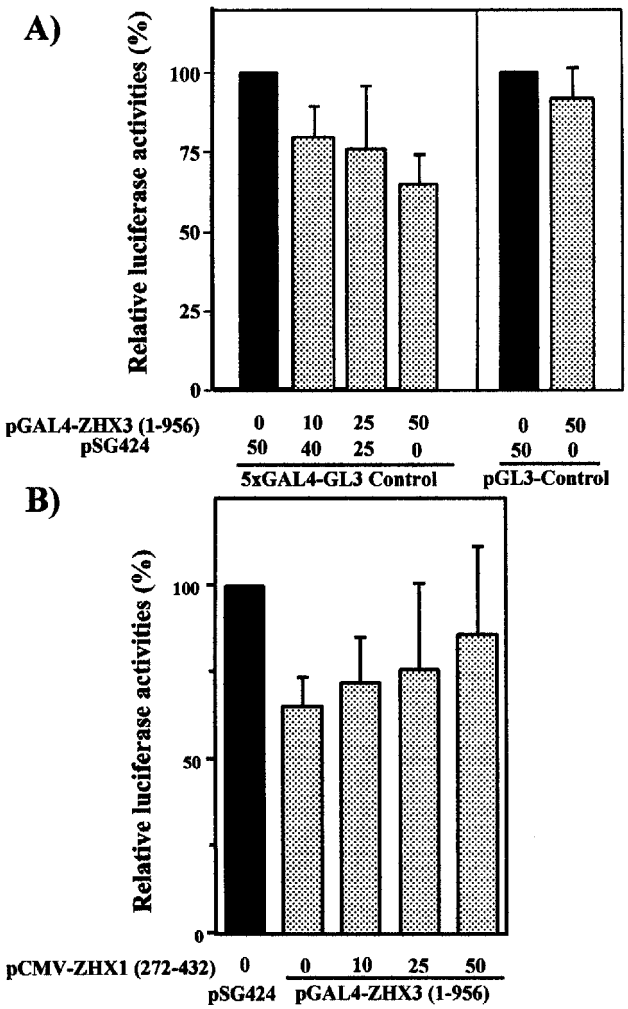

Figure 6 ZHX3 is a transcriptional repressor

(**A**) HEK-293 cells were co-transfected with 2 ng of the pRL-CMV, 50 ng of the simian virus 40 (SV40) promoter-directed expression vector and 100 ng of the 5xGAL4-pGL3 Control or pGL3-Control reporter plasmid. pSG424 and pGAL4-ZHX3 (1-956) express GAL4 DBD alone and the entire coding sequence of human ZHX3 fused to the GAL4 DBD, respectively. A value of 100 % was assigned to the promoter activity for the reporter plasmid in the presence of 50 ng of pSG424. (**B**) HEK-293 cells were co-transfected with 2 ng of the pRL-CMV, 50 ng of the SV40 promoter-directed expression vector, 100 ng of the 5xGAL4-pGL3 Control reporter plasmid and the indicated amount of pCMV-ZHX1 (242-432) expression plasmid. The total amount of plasmid (202 ng) was adjusted by the addition of the pcDNA3.1His-C2, if necessary. A value of 100 % was assigned to the promoter activity of the reporter plasmid in the presence of 50 ng of pSG424 and 50 ng of pcDNA3.1His-C2. 48 h after transfection, cells were harvested and both firefly and sea pansy luciferase activities were determined. Firefly luciferase activities were normalized by the sea pansy luciferase activities in all experiments. Each column and bar represents the mean ± S.D. from at least five transfection experiments.

activity was decreased in a dose-dependent manner. The maximal inhibition was obtained with 50 ng of the pGAL4-ZHX1 (1-956). In contrast, when the pGL3-Control lacking five copies of the GAL4-binding sites was transfected with the pSG424 or pGAL4-ZHX3 (1-956), the luciferase activities remained unchanged (Figure 6A). These results show that the GAL4–ZHX3 fusion protein decreases luciferase activity in a GAL4-binding-site-dependent manner, indicating that ZHX3 acts as a transcriptional repressor.

We then examined the issue of whether heterodimerization of ZHX3 with ZHX1 is required for its transcriptional repressor activity. We prepared the pCMV-ZHX1 (272-432), in which

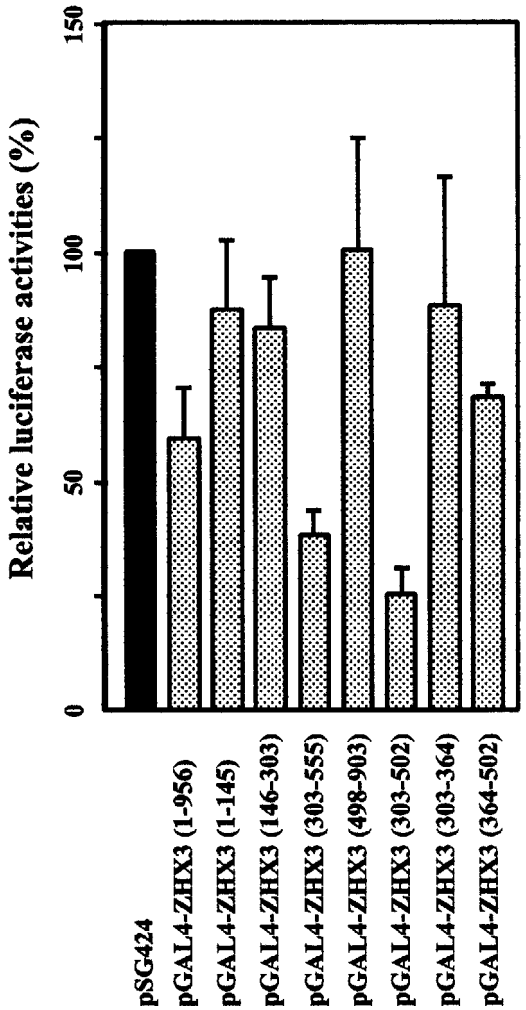

Figure 7 Determination of the minimal repressor domain of ZHX3

The pSG424 and various pGAL4-ZHX3 constructs expressing GAL4 DBD alone and various deletion mutants of human ZHX3 fused to the GAL4 DBD were used. Conditions were the same as described for Figure 6(A). Each column and bar represents the mean ± S.D. from at least five transfection experiments.

amino acids 272–423 of ZHX1 are expressed. Although this region corresponds to the dimerization domain of ZHX1 with ZHX3, it does not contain the repressor domain of ZHX1 [12]. Therefore, the overexpression of this protein functions as a dominant-negative form of ZHX1. When the plasmid was co-transfected in the above assay system, the luciferase activity was increased in a dose-dependent manner (Figure 6B). In contrast, co-transfection of the pcDNA3.1HisC-2 had no effect on luciferase activity. These results suggest that heterodimerization of ZHX3 with ZHX1 is a prerequisite for repressor activity.

Finally, to determine the minimal repressor domain of ZHX3, 5xGAL4-pGL3 Control was transfected with various plasmids, pGAL4-ZHX3 (1-145), pGAL4-ZHX3 (146-303), pGAL4-ZHX3 (303-555) or pGAL4-ZHX3 (498-903) (Figure 7). Only pGAL4-ZHX3 (303-555), which expresses amino acids 303-555, led to a decrease in luciferase activity. For a more detailed analysis, we prepared the effector plasmids pGAL4-ZHX3 (303-502), pGAL4-ZHX3 (303-364) and pGAL4-ZHX3 (364-502). Only when pGAL4-ZHX3 (303-502) was transfected with the reporter plasmid did the luciferase activity decrease (Figure 7). These results show that the amino acid sequence between residues 303 and 502 of ZHX3 are essential for repressor activity.

Determination of subcellular localization of ZHX3 and mapping of NLSs

To examine the subcellular localization of the ZHX3 protein, we employed the GFP–ZHX3 fusion-protein expression system. Various truncated forms of ZHX3 fused to GFP were prepared. These plasmids were transfected into HEK-293 cells and the subcellular localization of the GFP fusion proteins observed. pEGFP-C1E1, encoding GFP protein alone, was observed in the whole cell (Figure 8). In contrast, GFP–ZHX3 (1-956), in which full-length ZHX3 was fused to the C-terminus of GFP, was localized in the nuclei. To determine the NLS of ZHX3, various plasmids were transfected. When pGFP-ZHX3 (1-303), pGFP-ZHX3 (303-555) and pGFP-ZHX3 (555-956) were transfected both pGFP-ZHX3 (1-303) and pGFP-ZHX3 (303-555) were located in the nuclei. In contrast, when pGFP-ZHX3 (555-956) was transfected, the protein was localized outside of the nuclei. These results suggest that ZHX3 contains two NLS and a nuclear export signal. To map the minimal NLSs, various plasmids were constructed. Only when three plasmids, pGFP-ZHX3 (1-107), pGFP-ZHX3 (364-555) and pGFP-ZHX3 (497-555), were transfected was the nuclear localization of ZHX3 observed. These results show that ZHX3 is able to localize in the nuclei as a GFP fusion protein, and that two NLSs of ZHX3 are located in amino acids 1–107 and 497–555.

DISCUSSION

We conducted a search for ZHX1-interacting proteins, mainly by analysing a novel transcriptional repressor of them, ZHX3, and mapped its functional domains. The minimal functional domains of ZHX3 are summarized in Figure 9. ZHX3 as well as ZHX1 contains two Znf motifs and five HDs, forms a homodimer, interacts with the AD of NF-YA, and is localized in the nucleus. In addition, ZHX3 mRNA is expressed ubiquitously. From these findings, we conclude that both ZHX1 and ZHX3 are members of the same family, namely the ZHX family.

While the similarity of the entire amino acid sequences of ZHX1 and ZHX3 was 34.4%, the two Znf motifs and five HDs were highly conserved. Similarities in the amino acid sequences of Znf1, Znf2, HD1, HD2, HD3, HD4 and HD5 between ZHX1 and ZHX3 were 50.0, 45.5, 61.7, 50.0, 53.3, 43.3 and 33.3%, respectively. The HD4 showed a much lower similarity than the other domains. A unique glutamic-acid-rich acidic region is located in the amino acid sequence between residues 670 and 710 of ZHX3 (Figures 1 and 9). Generally, the Znf motif, the HD and the acidic region are responsible for the functional properties of the transcription factor. For example, both the Znf motif and HD, which consist of 60 amino acids, are required for binding to the cognate DNA sequence, the glutamic-acid-rich regions are involved in transcriptional activity, and the basic region is the DBD or NLS [11,14,27–30].

ZHX3 not only forms a heterodimer with ZHX1 but also forms a homodimer. Amino acids 242–488 of ZHX3 are necessary and sufficient for these dimerizations (Figures 3 and 4). A minimal domain for the homo- and hetero-dimerization of ZHX1 with ZHX3 was mapped to amino acids 272–432 of ZHX1 (Figure 3 and [12]). These regions include the HD1 but HD1 alone failed to dimerize (Figures 3–5). A more extensive region including

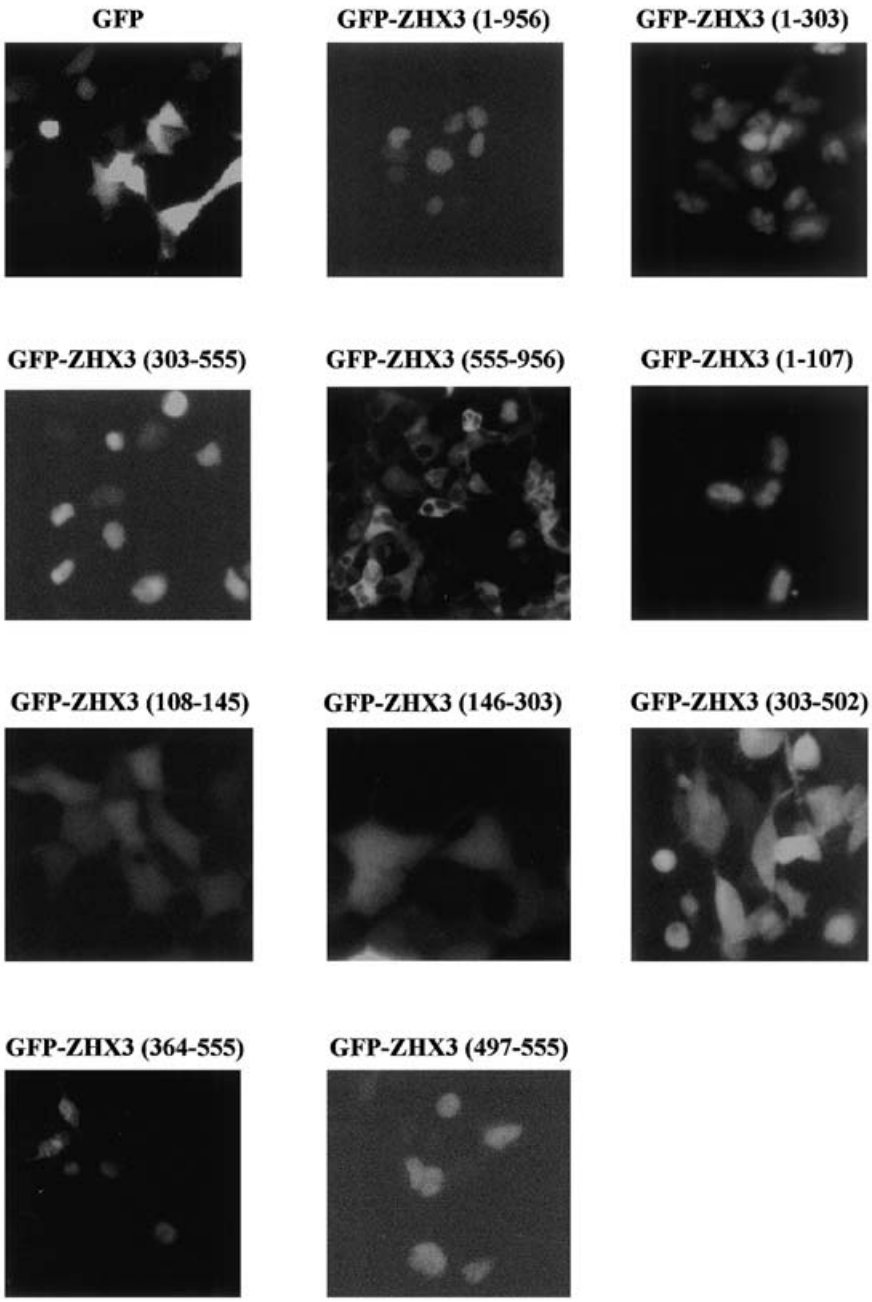

Figure 8 Subcellular localization of ZHX3 in HEK-293 cells and determination of NLSs

Expression plasmids (300 ng) encoding GFP alone or various truncated ZHX3 proteins fused to the C-terminus of GFP were transfected into HEK-293 cells. At 48 h after transfection, the subcellular localization of GFP fusion proteins was observed. Constructs are given at the top of each panel.

HD1 is required for dimerization. Furthermore, both ZHX3 and ZHX1 interact with the AD of NF-YA; the former interacts with a serine/threonine-rich AD and the latter with a glutamine-rich AD of the NF-YA, respectively (Figure 5 and [7]). An interaction domain of ZHX3 with the AD of NF-YA was mapped to the same region as the dimerization domain of ZHX3 (Figure 5). In contrast, the amino acid sequence between 272 and 564, which contains the HD1–HD2 region of human ZHX1, is required for its interaction [7]. The issue of whether a heterodimer complex of ZHX1 with ZHX3 interacts with different ADs of NF-YA remains to be determined.

ZHX3 is a transcriptional repressor (Figures 6 and 7). The minimal repressor domain of ZHX3 is mapped to an overlapping region with both dimerization and interaction domains. Interestingly, the overexpression of the heterodimerization domain of ZHX1, which is not responsible for repressor activity, led to a decrease in the repressor activity of ZHX3 (Figure 6B). This raises the possibility that ZHX3 itself has no repressor activity and that the observed activity is dependent upon the repressor activity of a dimerization partner, ZHX1, in which the repressor domain is located in the C-terminus of the acidic region [12]. However, it cannot be ruled out that the dimerization domain

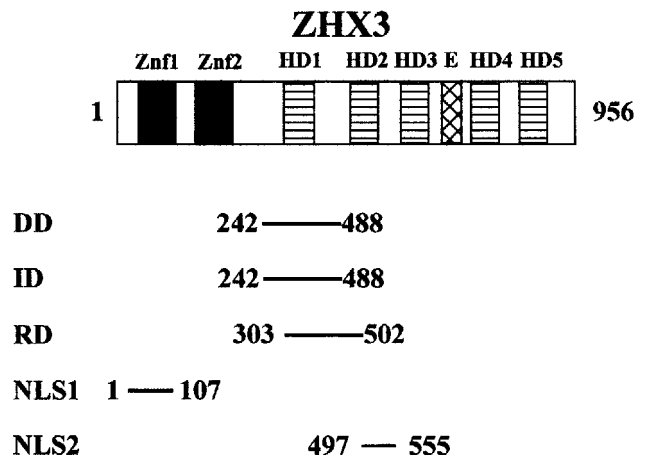

Figure 9 Schematic diagram of the functional domains of human ZHX3

E, glutamic acid-rich region; DD, dimerization domain; ID, interaction domain with NF-YA; RD, repressor domain.

of ZHX3 has *bona fide* repressor activity. It is unclear whether ZHX3 is a DNA-binding protein or not. As a result, it appears that a region of ZHX3 including the HD1 region is a pleiotropic domain; a homo- and hetero-dimerization domain with ZHX1, an interaction domain with the AD of NF-YA, and a repressor domain.

Regions of transcriptional regulation interact with cofactors to function as transcriptional repressors [31,32]. These cofactors include mSin3A/B, histone deacetylases and the nuclear co-repressor (N-CoR)/silencing mediator of receptor transcription. As ZHX1-interacting proteins we cloned two co-repressors, BS69 and ATF-IP (Table 1) [19,22]. BS69 was first identified as a protein that interacts directly with the AD of the 289R adenovirus type 5 E1A protein [19]. It has been also reported that BS69 mediates repression, at least in part, through an interaction of the MYND domain of BS69 with the co-repressor N-CoR [33]. In contrast, ATF-IP interacts with several components of the basal transcription machinery (TFIIE and TFIIH), including RNA polymerase II holoenzyme [22]. When ZHX1 and ZHX3 act as a transcriptional repressor, it could interact with these co-repressors, thus repressing gene transcription.

Furthermore, both ZHX1 and ZHX3 are NF-YA-interacting proteins. It has been reported that NF-Y is associated with co-activators, p300 and p300/cAMP response element-binding protein-binding protein-associated factor (P/CAF) [1]. In particular, P/CAF with histone acetyltransferase activity interacts with the NF-YA to form a transcriptionally active NF-Y complex [1]. Therefore, it is likely that combinations of interactions among ZHX1, ZHX3 and NF-YA affect the transcriptional activity of NF-Y. For example, either ZHX1 or ZHX3, or both, may enhance or interfere with the association of P/CAF with the NF-Y, thus regulating NF-Y activity. In addition, the transcriptional repressor, a member of the ZHX family, and a co-repressor are able to directly associate with the NF-YA, thus inhibiting NF-Y activity. In any case, it is possible that the ZHX proteins participate in the regulation of a number of NF-Y-regulatable genes.

Although ZHX3 mRNA is expressed ubiquitously, it was found to be expressed more highly in skeletal muscle, kidney and testis (Figure 2). The size of ZHX3 mRNA varied as determined by Northern blot analysis. The cloned insert contains 9302 bp and the size is the same as the largest transcript of ZHX3. When a search for the human *ZHX3* gene was conducted using the database compiled by the Human Genome Project, it was found to be located in chromosome 20q. This suggests that the *ZHX3* gene exists as a single copy per haploid human genome. The nucleotide sequence of ZHX3 cDNA revealed that multiple polyadenylation signals exist in the 3′-non-coding region. Therefore, it is likely that smaller mRNAs might be produced by the use of different polyadenylation signals from a single gene rather than by the existence of other ZHX3-related mRNAs.

When the entire coding region of ZHX3 was fused to the C-terminal end of the GFP, it became localized in the nuclei (Figure 8). There were two NLSs of ZHX3, amino acids 1–107 and 497–555. On the other hand, amino acids 498–956 of ZHX3 fused to GFP become exclusively localized not in the entire cell but external to the nucleus. GFP alone or the GFP–ZHX1 fusion protein lacking the NLS was localized to entire cells (Figure 8 and [12]). This indicates that this region of ZHX3 contains a nuclear-export signal. Therefore, ZHX3 is a more complicated protein that contains two NLSs and a nuclear-export signal in one molecule. In many other proteins, including ZHX1, it has been reported that the NLS was mapped to a cluster of basic amino acid residues [12,34]. This region is associated with nuclear-importing proteins such as importin α and is then translocated from the cytoplasm to the nuclei [28]. However, ZHX3 may associate with other molecules in order to be translocated to the nuclei, since the two NLSs of ZHX3 are not located in the basic region and do not exhibit any similarity with previously reported NLS.

We also cloned some ZHX1-interacting proteins differing from members of the ZHX family (Table 1). The isolated clones in Table 1 are not all confirmed. The issue of the nature of the biological significance of these interactions remains to be determined. Further studies will be required to completely understand the biological role of the ZHX family and its interactions with ZHX1-interacting proteins.

We are grateful to Dr Takahiro Nagase of the Kazusa DNA Research Institute (Chiba, Japan) for providing plasmid pBSII-KIAA0395. We are also grateful to Naoka Shimada, Kaoru Matsuura, Yoshiko Inoue and Miyuki Nakagawa for technical assistance. This investigation was supported by grants from the ONO Foundation, the Ichiro Kanehara Foundation, the Suzuken Memorial Foundation, Ministry of Education, Science, Sports and Culture of Japan and CREST of JST (Japan Science and Technology).

REFERENCES

1 Mantovani, R. (1999) The molecular biology of the CCAAT-binding factor NF-Y. Gene **239**, 15–27
2 Hu, Q. and Maity, S. N. (2000) Stable expression of a dominant negative mutant of CCAAT binding factor/NF-Y in mouse fibroblast cells resulting in retardation of cell growth and inhibition of transcription of various cellular genes. J. Biol. Chem. **275**, 4435–4444
3 Yamada, K. and Noguchi, T. (1999) Nutrient and hormonal regulation of pyruvate kinase gene expression. Biochem. J. **337**, 1–11
4 Yamada, K. and Noguchi, T. (1999) Regulation of pyruvate kinase M gene expression. Biochem. Biophys. Res. Commun. **256**, 257–262
5 Wang, Z., Takenaka, M., Imai, E., Yamada, K., Tanaka, T. and Noguchi, T. (1994) Transcriptional regulatory regions for expression of the rat pyruvate kinase M gene. Eur. J. Biochem. **220**, 301–307
6 Yamada, K., Tanaka, T., Miyamoto, K. and Noguchi, T. (2000) Sp family members and nuclear factor-Y cooperatively stimulate transcription from the rat pyruvate kinase M gene distal promoter region via their direct interactions. J. Biol. Chem. **275**, 18129–18137
7 Yamada, K., Osawa, H. and Granner, D. K. (1999) Identification of proteins that interact with NF-YA. FEBS Lett. **460**, 41–45
8 Barthelemy, I., Carramolino, L., Gutierrez, J., Barbero, J. L., Marquez, G. and Zaballos, A. (1996) zhx-1: a novel mouse homeodomain protein containing two zinc-fingers and five homeodomains. Biochem. Biophys. Res. Commun. **224**, 870–876
9 Yamada, K., Printz, R. L., Osawa, H. and Granner, D. K. (1999) Human ZHX1: cloning, chromosomal location, and interaction with transcription factor NF-Y. Biochem. Biophys. Res. Commun. **261**, 614–621

10 Hirano, S., Yamada, K., Kawata, H., Shou, Z., Mizutani, T., Yazawa, T., Kajitani, T., Sekiguchi, T., Yoshino, M., Shigematsu, Y. et al. (2002) Rat zinc-fingers and homeoboxes 1 (ZHX1), a nuclear factor-YA-interacting nuclear protein, forms a homodimer. Gene **290**, 107–114
11 Gehring, W. J., Affolter, M. and Burglin, T. (1994) Homeodomain proteins. Annu. Rev. Biochem. **63**, 487–526
12 Yamada, K., Kawata, H., Matsuura, K., Shou, Z., Hirano, S., Mizutani, T., Yazawa, T., Yoshino, M., Sekiguchi, T., Kajitani, T. and Miyamoto, K. (2002) Functional analysis and the molecular dissection of zinc-fingers and homeoboxes 1 (ZHX1). Biochem. Biophys. Res. Commun. **279**, 368–374
13 Sadowski, I. and Ptashne, M. (1989) A vector for expressing GAL4(1–147) fusions in mammalian cells. Nucleic Acids Res. **17**, 7539
14 Tanaka, T., Inazu, T., Yamada, K., Myint, Z., Keng, V. W., Inoue, Y., Taniguchi, N. and Noguchi, T. (1999) cDNA cloning and expression of rat homeobox gene, *Hex*, and functional characterization of the protein. Biochem. J. **339**, 111–117
15 Inazu, T., Yamada, K. and Miyamoto, K. (1999) Cloning and expression of pleckstrin 2, a novel member of the pleckstrin family. Biochem. Biophys. Res. Commun. **265**, 87–93
16 Yamada, K., Mizutani, T., Shou, Z., Yazawa, T., Sekiguchi, T., Yoshino, M., Inazu, T. and Miyamoto, K. (2001) Cloning and functional expression of an E box-binding protein from rat granulosa cells. Biol. Reprod. **64**, 1315–1319
17 Yamada, K., Wang, J.-C., Osawa, H., Scott, D. K. and Granner, D. K. (1998) Efficient large-scale transformation of yeast. BioTechniques **24**, 596–600
18 Ausubel, F. M., Brent, R., Kingston, R. E., Moore, D. D., Seidman, J. G., Smith, J. A. and Struhl, K. (eds) (1994) *Saccharomyces cerevisiae*. In Current Protocols in Molecular Biology, pp. 13.6.1–13.6.6, John Wiley and Sons, New York
19 Hateboer, G., Gennissen, A., Ramos, Y. F. M., Kerkhoven, R. M., Sonntag-Buck, V., Stunnenberg, H. G. and Bernards, R. (1995) BS69, a novel adenovirus E1A-associated protein that inhibits E1A transactivation. EMBO J. **14**, 3159–3169
20 Byrd, P. J., Cooper, P. R., Stankovic, T., Kullar, H. S., Watts, G. D. J., Robinson, P. J. and Taylor, A. M. R. (1996) A gene transcribed from the bidirectional ATM promoter coding for a serine rich protein: amino acid sequence, structure and expression studies. Hum. Mol. Genet. **5**, 1785–1791
21 Nishi, N., Shoji, H., Miyanaka, H. and Nakamura, T. (2000) Androgen-regulated expression of a novel member of the aldo-keto reductase superfamily in regrowing rat prostate. Endocrinology **141**, 3194–3199
22 DeGraeve, F., Bahr, A., Chatton, B. and Kedinger, C. (2000) A murine ATFa-associated factor with transcriptional repressing activity. Oncogene **10**, 1807–1819
23 Gossen, M., Schmitt, I., Obst, K., Wahle, P., Epplen, J. T. and Riess, O. (1996) cDNA cloning and expression of *rsca1*, the rat counterpart of the human spinocerebellar ataxia type 1 gene. Hum. Mol. Genet. **5**, 381–389
24 Macalma, T., Otte, J., Hensler, M. E., Bockholt, S. M., Louis, H. A., Kalff-Suske, M., Grzeschik, K.-H., von der Ahe, D. and Beckerle, M. C. (1996) Molecular characterization of human zyxin. J. Biol. Chem. **271**, 31470–31478
25 Nishiyama, C., Takahashi, K., Nishiyama, M., Okumura, K., Ra, C., Ohtake, Y. and Yokota, T. (2000) Polymorphism of transcription factor Elf-1 affecting its regulatory function in transcription. Biosci. Biotechnol. Biochem. **64**, 2601–2607
26 Thirman, M. J., Diskin, E. B., Bin, S. S., Ip, H. S., Miller, J. M. and Simon, M. C. (1997) Developmental analysis and subcellular localization of the murine homologue of ELL. Proc. Natl. Acad. Sci. U.S.A. **94**, 1408–1413
27 White, J. H., Brou, C., Wu, J., Burton, N., Egly, J., M. and Chambon, P. (1991) Evidence for a factor required for transcriptional stimulation by the chimeric acidic activator GAL-VP16 in HeLa cell extracts. Proc. Natl. Acad. Sci. U.S.A. **88**, 7674–7678
28 Kaffman, A. and O'Shea, E. K. (1999) Regulation of nuclear localization: a key to a door. Annu. Rev. Cell Dev. Biol. **15**, 291–339
29 Philipsen, S. and Suske, G. (1999) A tale of three fingers: the family of mammalian Sp/XKLF transcription factors. Nucleic Acids Res. **27**, 2991–3000
30 Guiral, M., Bess, K., Goodwin, G. and Jayaraman, P. S. (2001) PRH represses transcription in hematopoietic cells by at least two independent mechanisms. J. Biol. Chem. **276**, 2961–2970
31 Hu, X. and Lazar, M. A. (2000) Transcriptional repression by nuclear hormone receptors. Trends Endocrinol. Metab. **11**, 6–10
32 Wolffe, A. P., Urnov, F. D. and Guschin, D. (2000) Co-repressor complexes and remodelling chromatin for repression. Biochem. Soc. Trans. **28**, 379–386
33 Masselink, H. and Bernards, R. (2000) The adenovirus E1A binding protein BS69 is a corepressor of transcription through recruitment of N-CoR. Oncogene **19**, 1538–1546
34 Mattaj, I. W. and Englmeier, L. (1998) Nucleocytoplasmic transport: the soluble phase. Annu. Rev. Biochem. **67**, 265–306

Received 2 December 2002/28 February 2003; accepted 27 March 2003
Published as BJ Immediate Publication 27 March 2003, DOI 10.1042/BJ20021866